

Mechanical properties study of micro- and nano-hydroxyapatite reinforced ultrahigh molecular weight polyethylene composites

Xueqin Kang, Wei Zhang, Chunmin Yang

China University of Mining and Technology, Xuzhou, Jiangsu 221116, China

Correspondence to: C. Yang (E-mail: ychm_cumt@163.com)

ABSTRACT: This is a comparative study between ultrahigh molecular weight polyethylene (UHMWPE) reinforced with micro- and nano-hydroxyapatite (HA) under different filler content. The micro- and nano-HA/UHMWPE composites were prepared by hot-pressing method, and then compression strength, ball indentation hardness, creep resistance, friction, and wear properties were investigated. To explore mechanisms of these properties, differential scanning calorimetry, infrared spectrum, wettability, and scanning electron microscopy with energy dispersive spectrometry analysis were carried out on the samples. The results demonstrated that UHMWPE reinforced with micro- and nano-HA would improve the ball indentation hardness, compression strength, creep resistance, wettability, and wear behavior. The mechanical properties for both micro- and nano-HA/UHMWPE composites were comparable with pure UHMWPE. The mechanical properties of nano-HA/UHMWPE composites are better compared with micro-HA/UHMWPE composites and pure UHMWPE. The optimum filler quantity of micro- and nano-HA/UHMWPE composites is found to be at 15 wt % and 10 wt %, separately. The micro- and nano-HA/UHMWPE composites exhibit a low friction coefficient and good wear resistance at this content. The worn surface of HA/UHMWPE composites shows the wear mechanisms changed from furrow and scratch to surface rupture and delamination when the weight percent of micro- and nano-HA exceed 15 wt % and 10 wt %. © 2015 Wiley Periodicals, Inc. *J. Appl. Polym. Sci.* **2016**, *133*, 42869.

KEYWORDS: composites; friction; mechanical properties; nanoparticles; nanowires and nanocrystals; properties and characterization; wear and lubrication

Received 12 March 2015; accepted 24 August 2015

DOI: 10.1002/app.42869

INTRODUCTION

Ultrahigh molecular weight polyethylene (UHMWPE) is a type of polyethylene (PE) with extremely high molecular weight (more than 1×10^6 g/mol) and possesses the highest wear resistance, better biocompatibility, lower friction, better chemical inertness, and higher impact resistance compared with any other polymers.^{1–3} UHMWPE has been used as bio-medical material for an acetabular prosthesis component in hip and knee total joint replacement, engineering bearing, valves, and automotive.^{4–7} The use of UHMWPE has been limited by its low Young's modulus, low load bearing, and antifatigue capacity. To overcome these problems, UHMWPE composites were fabricated by adding reinforced particles and fiber fillers to improve its mechanical and tribological properties. The additives include carbon fiber,⁸ kaolin,⁷ natural coral particles,⁹ zirconium particles,⁶ TiO₂,¹⁰ Al₂O₃,¹¹ carbon nanotubes,¹² etc. Studies have shown that the addition of an optimum amount of micro- and nano-scale of fibers, inorganic particles, ceramic, and biomaterial with UHMWPE matrix would significantly reduce the wear rate under sliding wear conditions.¹³

The studies of UHMWPE composites in abrasive wear conditions are extensively investigated by many researchers. Tai *et al.*¹⁴ reported that UHMWPE filled with grapheme oxide nanosheets improved its wear resistance. Cao *et al.*¹⁵ also reported that wear resistance of UHMWPE was effectively enhanced after reinforced with basalt fibers. Ren *et al.*¹⁶ studied the mechanical and abrasive wear resistance of UHMWPE was improved upon the addition of quartz sand.

It is important to note that the filler loadings, filler-matrix interaction, dispersion of the fillers in the composites, type of fillers, filler's size and shape are crucial in determining the mechanical and wear behavior of the composites.^{13,17} Hydroxyapatite (HA) was used as the filler in this research since it exhibits excellent mechanical properties, biocompatibility, and bioactivity. HA is similar to bone minerals in composition, size, crystal structure, and morphology.^{18–20} Fang *et al.*²¹ reported that nano-HA/UHMWPE composites exhibited a significant enhancement of stiffness without decreasing the yield strength and ductility of UHMWPE. Although numerous researches

have used HA reinforced polymeric material to improve its mechanical and tribological properties, the implementation of micro- and nano-scale HA in UHMWPE composites not been extensively studied. The addition of HA into the UHMWPE would not only enhance the tribological properties, but also induces additional biocompatibility and bioactivity, which may be useful in implant materials.

MATERIALS AND EXPERIMENTAL

Materials

Micro- and nano-HA particles were provided by Shanghai Hualan Chemical Technology Co., Ltd., China, with an average diameter of 12 μm and 20 nm. UHMWPE powder GUR 4150 (molecular weight 9×10^6 g/mol) was supplied by SCM Industrial Chemical Co. Ltd., China. Silane coupling agent (γ -aminopropyl triethoxysilane, trade name: KH550) was purchased from Shanghai Wenhua Chemical Pigment Co. Ltd., China. It was used to introduce reactive functional groups on the surface of HA particles.

Surface Modification of Micro- and Nano-HA

The silane coupling agent was dissolved in aqueous ethanol solution containing 140 mL of ethanol and 10 mL of deionized water. The solution was stirred for half an hour and then micro- or nano-HA was added. The mixture was dispersed in ultrasonic cleaner for 3 min, and then stirred for 3 h with mechanical stirring. The pH of the mixture was adjusted to 9–10 by sodium hydroxide solution. The precipitate was collected and washed with ethanol to remove the byproducts, and then dried at 100°C under vacuum conditions for 24 h.

Specimen Preparation

Firstly 5, 10, 15 and 20 wt % of micro- and nano-HA were mixed homogeneously with UHMWPE using dry mechanical ball mill. The mixing process took 4 h to complete: 2 h each for both clockwise and anticlockwise direction. After mixing, the samples were preheated and hot pressed at a temperature of 200°C for 2 h and the test pressure was 15 MPa. The final product with dimensions (100 \times 100 \times 10) mm³ was obtained after cooling under room temperature. The roughness of the sample surface was measured with a contact-type roughness measuring instrument (JB-4C) and the value was no more than 0.08 μm .

Differential Scanning Calorimetric Analysis

To examine effects of micro- and nano-HA filling crystallinity, differential scanning calorimetry (DSC, Model: DSC-100) were performed on three specimens for each type of materials. The specimen about 40–50 mg was used in each measurement. An alumina pan was used in the sample cavity as a reference before the testing. All samples were heated from 30 to 200°C at 10°C/min. The total enthalpy of melting was calculated by integrating the endotherm curve from 50 to 160°C. The degree of crystallinity was calculated by dividing the value in enthalpy for the sample by 286.4 J/g, which is the theoretical heat of fusion for perfectly crystalline polyethylene.²² The melting temperature was determined by the peak point of the curve. To avoid the effect of heating on the experimental results, each specimen was only tested once. The results of three specimens for each type of materials were averaged.

Infrared Spectrum Analysis

To investigate the effects of filling and irradiation on molecular structure, UHMWPE, micro- and nano-HA/UHMWPE composites were analyzed under infrared absorption spectroscopy (VERTEX 80v, Bruker) using the pellet method. All measurements were performed from 500 to 4000 cm⁻¹ in the transmission mode, with a scan resolution of 4 cm⁻¹. To compare the materials, distinct absorption peaks were marked on spectrums.

Compression Property Characterization

The stress of wear-resisting material in actual use was commonly compression strength. The reference standard of compression experiment was Din EN ISO 604-2003. The sample of micro- and nano-HA/UHMWPE composites was (10 \times 10 \times 10) mm³. The test instrument was WDW-20 electronic universal testing machine and the test speed was 1 mm/min. The stress and strain were calculated using the following equations:

$$\sigma = P/A_0 \quad (1)$$

where σ is the stress, in MPa, P is the experimental load, in Newton, and A_0 is the original sectional area, in square meters.

$$\varepsilon = (L_0 - L)/L_0 \quad (2)$$

where ε is the strain, L is the length of the sample after deformation, in millimeter, and L_0 is the original length of the sample, in millimeter

Ball Indentation Hardness Test

To properly obtain the hardness of the micro- and nano-HA/UHMWPE composites, the experiment tested the ball indentation hardness of the HA/UHMWPE composites. The UMT tester (CETR, USA) was used to test the hardness and the test took the standard of ISO 2039-1:2003 as a reference. The indenter comprised a zirconia ceramic ball and the diameter of the ball was 5 mm. The initial load was 9.8 N and the test load was 49 N. Each sample was tested ten times and then averaged. Measured depths of impression and the ball indentation hardness could be calculated using the following equation:

$$H = \frac{0.21P_{\max}}{0.25\pi D h_{\max}} \quad (3)$$

Where P_{\max} is the test load, in Newton, on the indenter, D is the diameter of the ball indenter, in millimeter, and h_{\max} is the reduced depth of impression, in millimeter.

Creep Resistance Test

Visoelasticity is unique performance of UHMWPE and it will produce creep deformation in the process of force. Serious creep deformation will affect the precision of UHMWPE artificial joint and cause joint replacement failure. The creep behavior of materials, to some extent, can be reflected by indentation creep. So, the experiment tested the indentation creep resistance of the HA/UHMWPE composites. The indenter comprised a zirconia ceramic ball and the diameter of the ball was 5 mm. The constant load applied on the sample was 49 N for a period of 1 800 s. In the process of ball indentation, when the load was increased to 49 N, the indentation depth was set as 0 and the depth was noted.¹⁶ Each sample was tested five times and then averaged.

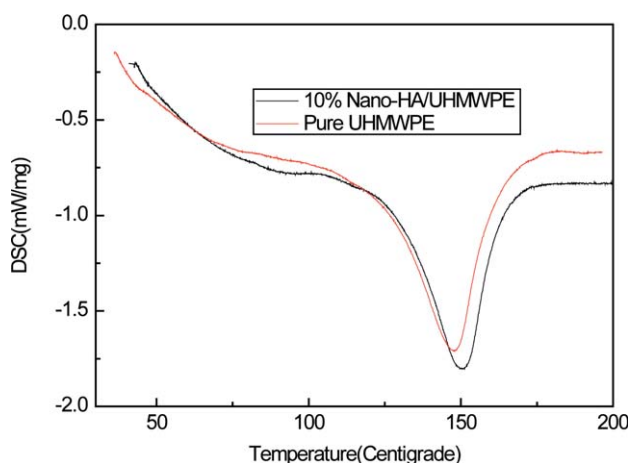


Figure 1. DSC curves of UHMWPE and 10 wt % nano-HA/UHMWPE samples. [Color figure can be viewed in the online issue, which is available at wileyonlinelibrary.com.]

Contact Angle Test

To simulate the body fluid environment,²³ bovine calf serum at room temperature was employed to deposit a 0.05 mL drop on the HA/UHMWPE composites surface. Contact angle measurement was carried out according to the sessile drop

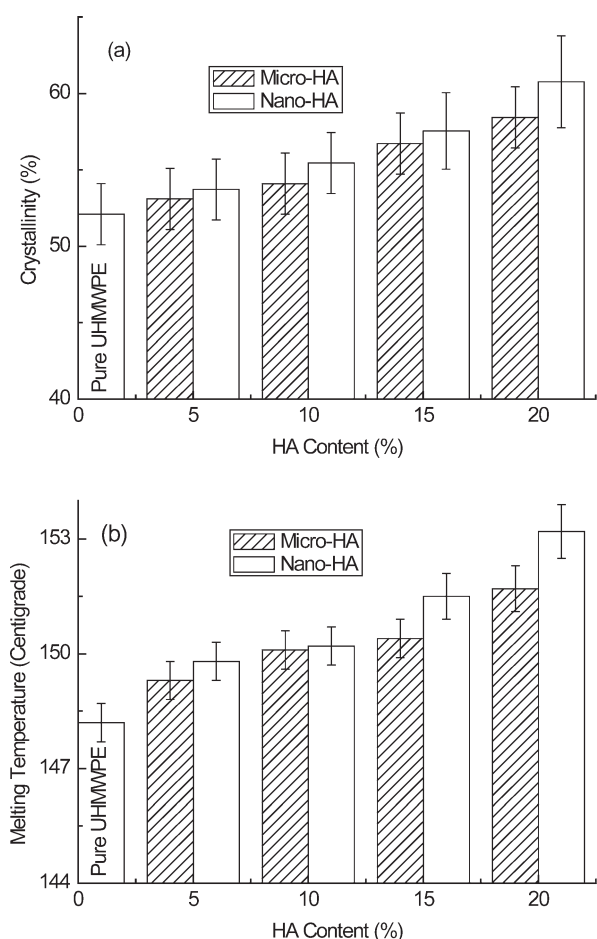


Figure 2. Results of DSC analysis: (a) crystallinity and (b) melting temperature as a function of filling content for micro- and nano-HA/UHMWPE samples.

technique and performed by the contact angle micrometer (JC2000B). The bovine calf serum drop was deposited accurately with a microsyringe on the sample surface. Each sample was tested ten times and then averaged.

Friction and Wear Test

Friction and wear test was performed on MM-200 friction tester using a block-on-ring test form. The test samples were cut from hot pressed molded samples into square specimens with dimensions of $(10 \times 10 \times 15) \text{ mm}^3$. The abrasion surface of the sample was $(10 \times 15) \text{ mm}^2$. The ring was made of GCr15 steel with the diameter of 50 mm and the thickness of 10 mm. All the rings were rubbed with fine sandpaper and polished with diamond polishing paste. The roughness value of the ring surface was $0.32 \mu\text{m}$. The test was carried out in the lubrication of bovine calf serum for 7200 s. The applied normal load was 198 N and the test speed was 200 r/min. The coefficient of friction was calculated by the following equation:

$$f = M / (R \cdot P) \quad (4)$$

Where, f is the coefficient of friction, M is the torque, in Nm, R is the radius of GCr15 steel ring, in meter, P is the vertical load of sample, in Newton.

Before and after wear test, each specimen was cleaned in an ethanol-filled ultrasonic bath and dried. The wear volume was taken as the wear parameter in this study, which was done on MicroXAM three-dimensional profilometer. Each sample was tested seven times and then averaged.

Scanning Electron Microscopy Analysis

To study mechanisms of wear, the worn surfaces were examined under scanning electron microscope (SEM, FEI Quanta TM 250). At least five specimens per group were used for the testing, and the typical image was chosen for every material. UHMWPE, micro- and nano-HA/UHMWPE composites surface was sputter coated with gold, and the sample chamber was drawn to low-vacuum with an accelerating voltage of 30 kV. Furthermore, energy dispersive spectrometry (EDS, Quanttax400-10, Bruker) was conducted on surfaces of filled materials.

RESULTS AND DISCUSSION

The characterization of HA/UHMWPE composites reveals the micro- and nano-HA particles have a strong influence on the mechanical properties of composite. A comparative study of micro- and nano-HA/UHMWPE composites against unfilled UHMWPE is presented.

Crystallinity Analysis

Typical DSC curves of UHMWPE and 10 wt % nano-HA/UHMWPE sample are shown in Figure 1 and results of crystallinity are shown in Figure 2. It can be seen that the crystallinity and melting temperature of filled micro- and nano-HA samples is higher than that of unfilled UHMWPE. The crystallinity and melting temperature increases with increasing content of micro- and nano-HA. At each filling content the melting temperature and crystallinity of nano-HA is higher than that of micro-HA filled samples. Previous study had demonstrated that filling

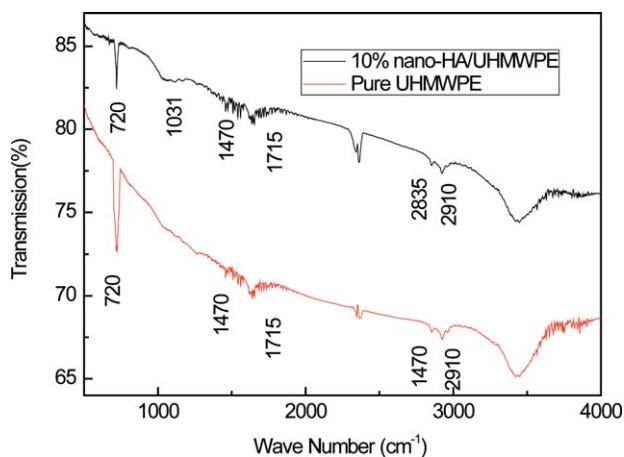


Figure 3. Results of IR analysis for UHMWPE and 10 wt % nano-HA/UHMWPE samples. [Color figure can be viewed in the online issue, which is available at wileyonlinelibrary.com.]

particles would increase crystallinity and melting temperature of polymer.²⁴

Infrared Spectrum Analysis

Typical infrared spectrum (IR) analysis curves are shown in Figure 3. At the wave number of 720 cm^{-1} , it is the rocking deformation of polyethylene²⁵ showing no difference among both samples. At the wave number of 1031 cm^{-1} , the orthophosphate group gives a broader band for nano-HA/UHMWPE sample. At the wave number of 1470 cm^{-1} , it is the bending deformation of polyethylene. Similar behavior could also be observed at the wave number of 2835 cm^{-1} and 2910 cm^{-1} , which are indicate of asymmetric stretching of $\text{CH}_3\text{-CH}_2\text{-}$ and symmetrical stretching of $\text{-CH}_2\text{-CH}_2\text{-}$ groups.²⁶ Furthermore, there are some absorption peaks at the wave number of 1715 cm^{-1} for both samples, which represent the wave number of carbonyl absorption peak. Thus, it indicates that there has an oxidation in UHMWPE and nano-HA/UHMWPE samples preparation. Oxidation can weaken the mechanical performance of UHMWPE,²⁷ so other sample preparation methods can be

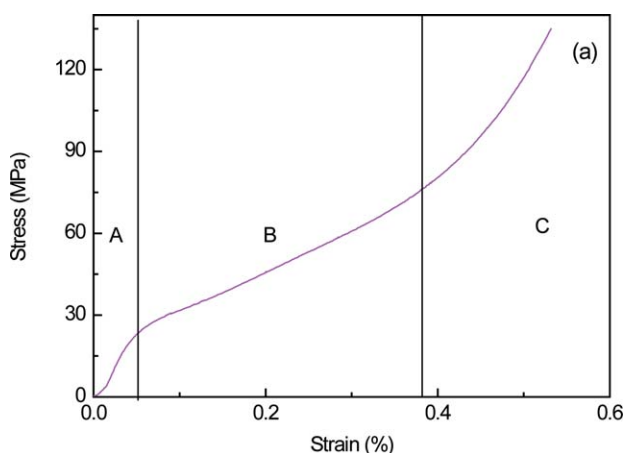


Figure 4. Typical stress–strain curve of UHMWPE and HA/UHMWPE samples. [Color figure can be viewed in the online issue, which is available at wileyonlinelibrary.com.]

taken to eliminate oxidation. Micro-HA has the same effect on UHMWPE as nano-HA.

Compression Properties

Figure 4 shows the typical stress–strain curves of HA/UHMWPE composites. From Figure 4 it is clearly observed that three regions corresponding to different stages of a compression test. Stage A is elastic stage, and at this stage the height of the sample gets short with the stress increasing, but the height restores to its original level when the stress removed completely. Stage B is steady creeping stage, at this stage the sample keeps on deformation with the stress increasing. Stress increase just because the cross section area of sample increases. The deformation can't restore to its original level when the stress removed completely. Stage C is the final rupture stage and this induce deformation non-uniformly, so the middle part of the sample presents cydariform and the stress increases rapidly.

Figure 5 shows the compression strength of UHMWPE and HA/UHMWPE composites under different content of HA particles. From Figure 5 we can see that the compression strength of micro- and nano-HA/UHMWPE composites shows a rising tendency with rising content of micro- and nano-HA from 5 wt % to 20 wt %. The reason for compression strength change can be concluded as follows: First, HA is much stronger than UHMWPE so composites with HA makes the UHMWPE stronger. Second, the reinforcement particles in a polymer matrix can impede the movement of UHMWPE molecular chain and hence improving the compression strength. Therefore, the improvement in compression properties is observed after the incorporation of micro- and nano-HA fillers into the UHMWPE matrix.

The compression strength of nano-HA/UMWPE composites is better than micro-HA/UMWPE composites and the deformation of nano-HA/UHMWPE composites in each stage is larger than that of micro-HA/UHMWPE with the same content of HA. This can be further supported by the comparative studies between nanoscale, microscale, and whisker shape of SiC fillers reinforced polymer composites which have been reported by Xue and Wang.²⁸ The found that nanoscale SiC as a filler in

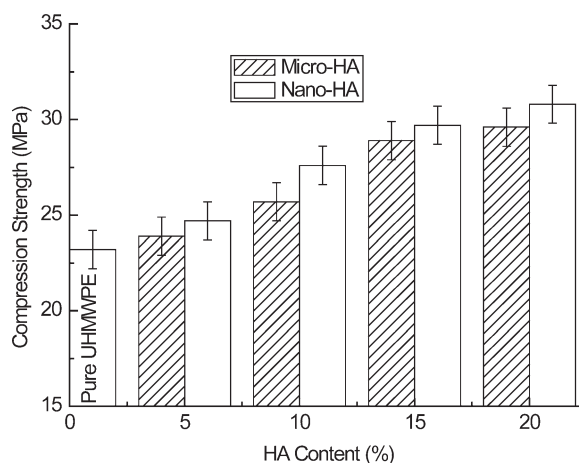


Figure 5. Compression strength as a function of filling content for micro- and nano-HA/UHMWPE samples.

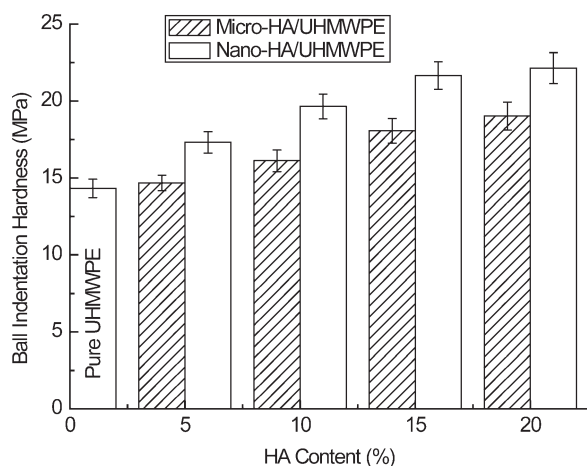


Figure 6. Ball indentation hardness as a function of filling content for micro- and nano-HA/UHMWPE samples.

polymer significantly improved the mechanical properties as compared with micro-sacle and whisker shape of SiC fillers. Therefore, it shows that the size of the fillers plays an important role in improving the compression strength of the polymer composites.

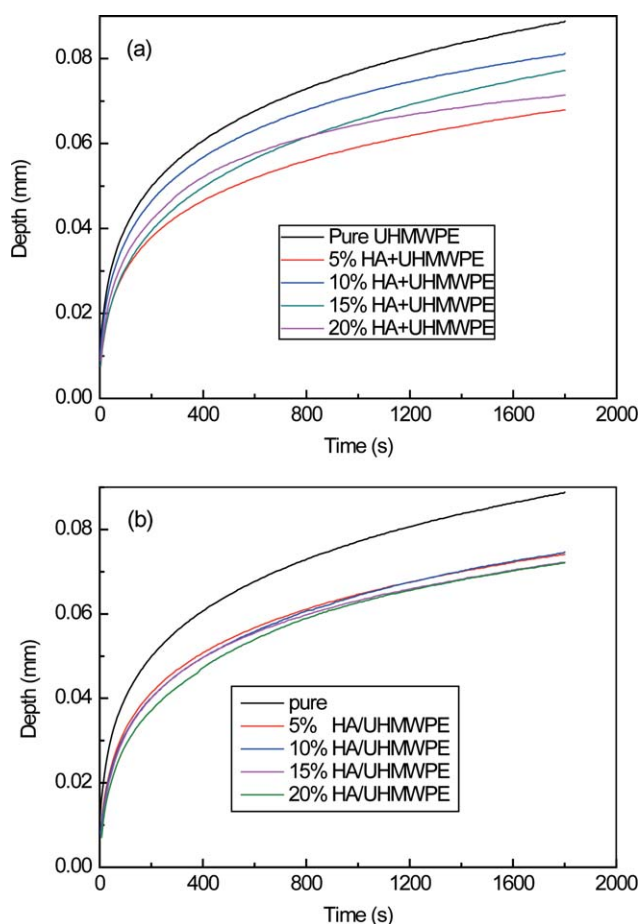


Figure 7. Indentation depth of (a) micro- and (b) nano-HA/UHMWPE samples as a function of time. [Color figure can be viewed in the online issue, which is available at wileyonlinelibrary.com.]

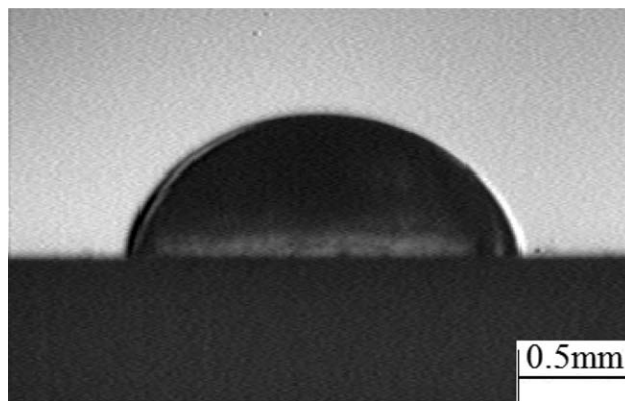


Figure 8. Microscopic picture of contact angle for HA/UHMWPE composites with bovine calf serum.

Hardness and Creep Resistance

Figure 6 shows the ball indentation hardness of micro- and nano-HA/UHMWPE composites under different content of HA particles. It is clearly observed that the filler addition increases the ball indentation hardness. The ball indentation hardness of pure UHMWPE is 14.32 MPa. The ball indentation hardness of micro-HA/UHMWPE composites is 14.66 MPa, 16.12 MPa, 18.06 MPa and 19.03 MPa at room temperature when the content of micro-HA particles is 5 wt %, 10 wt %, 15 wt %, and 20 wt %, separately. The ball indentation hardness of nano-HA/UHMWPE composites is 17.32, 19.64, 21.66, and 22.14 MPa at room temperature when the content of nano-HA particles is 5, 10, 15, and 20 wt %, separately. The ball indentation hardness of nano-HA/UHMWPE is higher than micro-HA/UHMWPE composites when they have the same HA content.

Figure 7 shows the creep resistance of micro- and nano-HA/UHMWPE composites. It can be seen from Figure 4 that the indentation depth of HA/UHMWPE composites increases drastically in the first 200s of the test and then increases slowly. The final indentation depth of micro-HA/UHMWPE composites reduces significantly with increasing content of micro-HA particles. The final indentation depth of nano-HA/UHMWPE

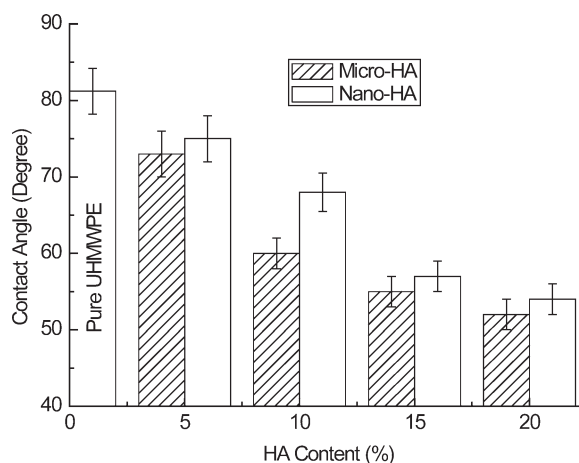


Figure 9. Contact angle as a function of filling content for micro- and nano-HA/UHMWPE samples.

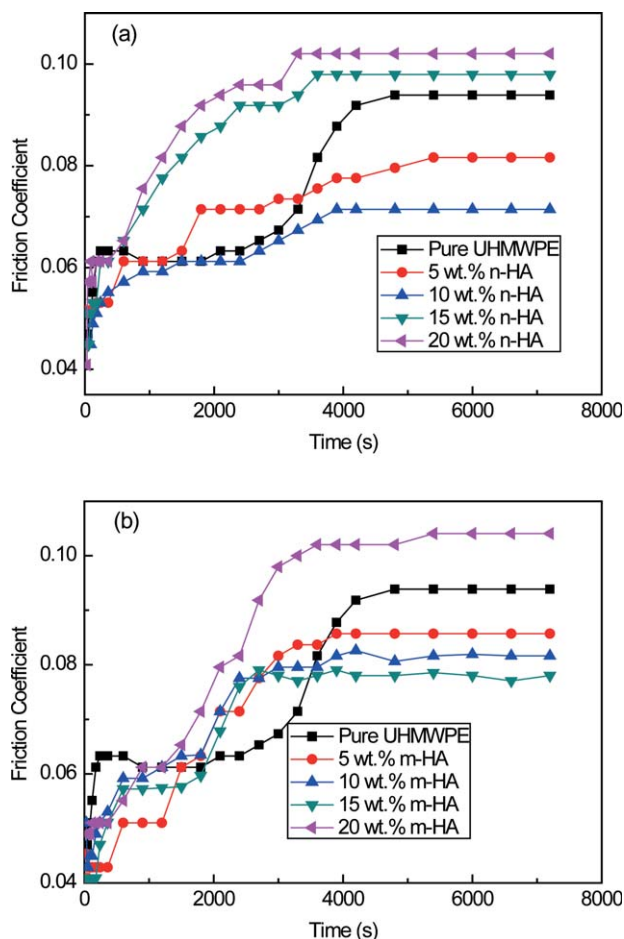


Figure 10. The friction coefficient of (a) micro- and (b) nano-HA/UHMWPE as a function of time. [Color figure can be viewed in the online issue, which is available at wileyonlinelibrary.com.]

composites reduces significantly when the content of nano-HA particles from 0 to 5 wt %, but it reduces, not obviously, when the content of nano-HA is more than 5 wt %. This can be explained by the close relationship between the hardness and creep resistance of the composites and the filler content. The filler embedded in the UHMWPE matrix and the distribution of fillers is uniform when the fillers quantity is below a certain amount.²⁹ Likewise, the dispersion of the fillers is poor when

the filler content is above the optimum amount i.e., around 10 wt % in this work. This is because at a higher filler content, the filler interparticle distance is reduced and particles tend to agglomerate.³⁰ The agglomeration of fillers would severe hardness and creep resistance. Therefore, the strength effect will reduce when the filler content above the optimum level.

The reason for ball indentation hardness and creep resistance change is similar to the change of compressive performance.

Wetting Properties

Figure 8 shows microscopic picture of the contact angle with bovine calf serum on HA/UHMWPE composites surface. Figure 9 shows the change of contact angle under different content of HA particles at room temperature. It can be seen from Figure 9 that contact angle of the composites decreases with the content of HA particles increasing. According to the change of contact angle, it can be seen that the wettability of HA/UHMWPE composites increases with increasing content of HA particles and the wettability of micro-HA/UHMWPE composites is better than that of nano-HA/UHMWPE composites, mainly because of the difference wettability of micro-HA, nano-HA particles and UHMWPE with calf serum.²⁶ It will be easy to form lubricating film on the friction surface when the sample has good wettability and then improve its friction and wear properties.

Friction and Wear Performance

Friction and wear property of composites is characterized by friction coefficient and wear volume. Figure 10 shows the variation of friction coefficient of HA/UHMWPE composites during wear test. All curves show an increasing tendency of friction coefficients as a function of testing time; friction coefficients have a stability value after 3 600 s. It can be seen that the stable friction coefficient of UHMWPE without adding HA is about 0.095. The stable friction coefficient of HA/UHMWPE composites decreases when the content of micro-HA increasing from 0 to 15 wt % and nano-HA increasing from 0 to 10 wt %, then the stable friction coefficient increases with the content of micro- and nano-HA particles increasing.

Figure 11 shows three dimension morphology of wear. Wear volume can be obtained according to the wear width because it was a circular arc and its diameter equals to the diameter of CoCrMo steel ring. Figure 12 shows the wear volume change with the content of micro- and nano-HA. The wear volume

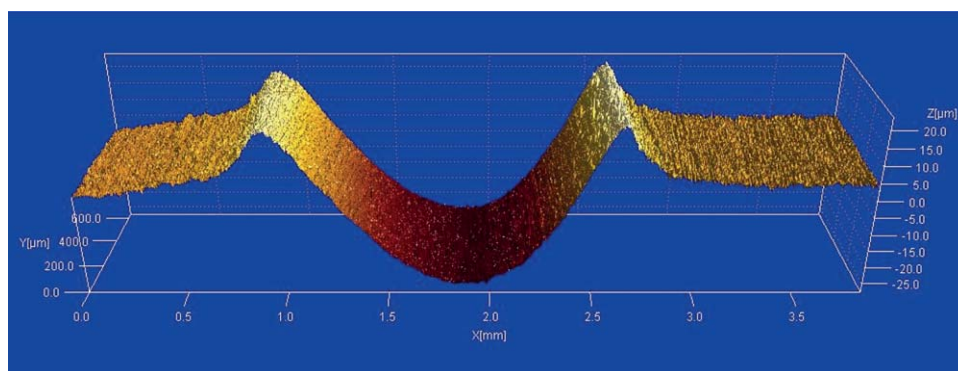


Figure 11. Three dimension morphology of wear surface. [Color figure can be viewed in the online issue, which is available at wileyonlinelibrary.com.]

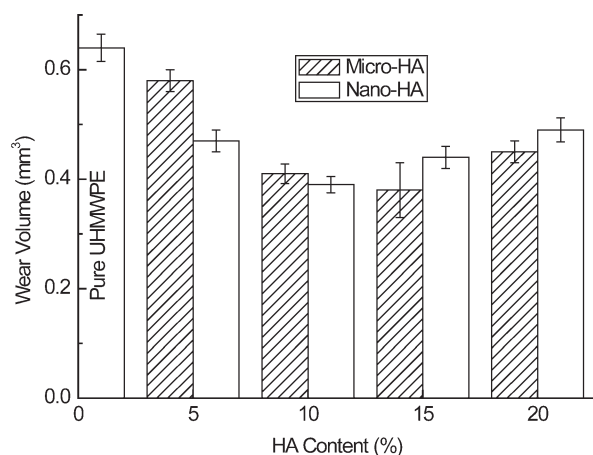


Figure 12. The wear volume as a function of filling content for micro- and nano-HA/UHMWPE samples.

decreases with the increase of HA particles content, but it increases when the content of micro- and nano-HA particles exceeds 15 wt % and 10 wt %. Figure 13 shows morphology of worn surfaces of UHMWPE and HA/UHMWPE composites, and EDS results of the areas, surrounded by black edges,

are shown in Figure 14. It can be seen from Figure 13 that the friction and wear mechanism is furrow and scratch in UHMWPE, micro- and nano-HA/UHMWPE composites. However, samples filled with more than 15 wt % micro-HA and 10 wt % nano-HA exhibit surface rupture and delamination. Bright spots are found on surface of all filled samples, especially for those filled with more than 15 wt % micro-HA and 10 wt % nano-HA. EDS results indicate that these spots are mainly composed of HA. UHMWPE filled with more HA results in a higher concentration of Ca.³¹

The enhanced wear resistance of filled HA samples when the content of micro- and nano-HA particles under 15 wt % and 10 wt % is mainly because two reasons. First, supporting function of filling particles on the contact surfaces, where filling HA particles could act as rigid spots against the counterface to reduce the normal load and shear stress of UHMWPE, resulting in a lower rate.³² Second, the wettability of UHMWPE is improved by HA particles and this enhances the wear resistance of HA/UHMWPE composites. To these reasons the more prominent supporting function and the increased mechanical properties would lead to a synergistic enhancement of wear resistance under the abrasive condition,

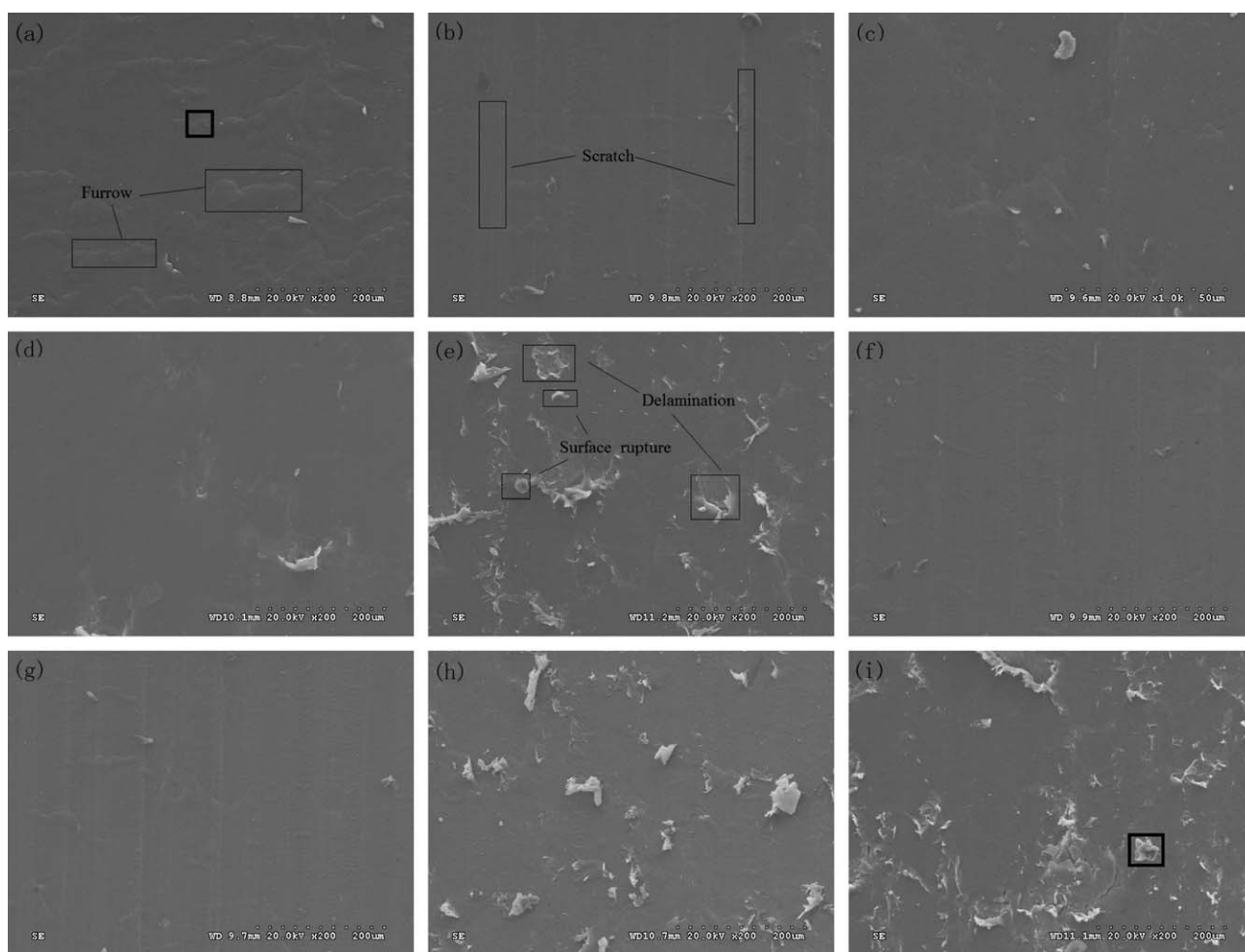


Figure 13. Wear morphology of (a) UHMWPE, UHMWPE samples reinforced with (b) 5 wt %, (c) 10 wt %, (d) 15 wt %, (e) 20 wt % micro-HA particles and (f) 5 wt %, (g) 10 wt %, (h) 15 wt %, (i) 20 wt % nano-HA particles.

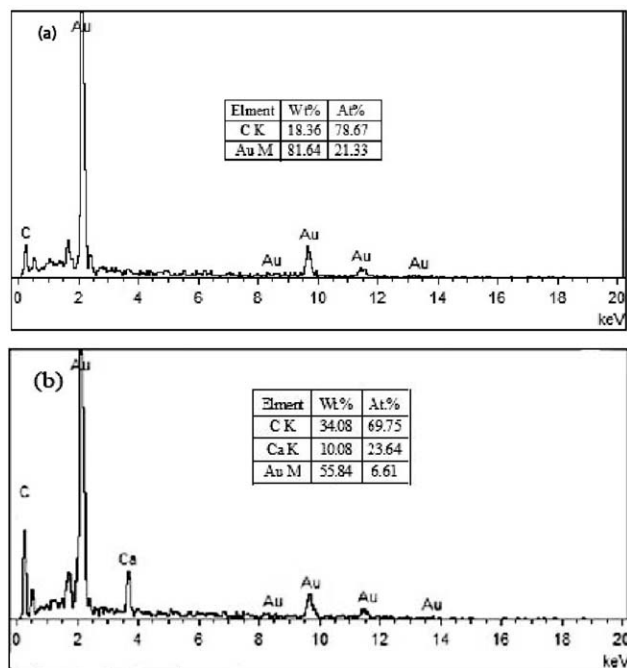


Figure 14. EDS results of worn surface for: (a) pure UHMWPE and (b) 15 wt % nano-HA/UHMWPE.

resulting in a lower wear rate than both UHMWPE and with lower content of micro- and nano-HA. Although a previous research pointed out that a brittle reinforced material with a higher hardness is prone to delaminate under *vivo* reciprocating loads.²⁷ When the filler reach to certain content, it may generate high stress concentration at the interfaces of fillers, so as to induce the delamination and reduce the friction and wear properties of micro- and nano-HA/UHMWPE.

CONCLUSION

The following conclusions are drawn from present study:

1. The compression strength, ball indentation hardness, creep resistance, crystallinity, and melting temperature of micro- and nano-HA/UHMWPE composites are improved with increasing content of micro- and nano-HA particles. These properties of nano-HA/UHMWPE composites are better or higher than micro-HA/UHMWPE composites with the same content of HA.
2. There are oxidation in UHMWPE and HA/UHMWPE samples preparation. The orthophosphate group gives a broader band for HA/UHMWPE around the wave number of 1031 cm^{-1} .
3. The contact angle of UHMWPE with bovine calf serum decreases with increasing content of micro- and nano-HA particles, so the wettability increases with the increase of content of micro- and nano-HA particles. The wettability of micro-HA/UHMWPE composites is better than nano-HA/UHMWPE composites with the same content of HA.
4. Friction coefficient and wear volume determined by wettability and surface morphology of micro- and nano-HA/UHMWPE composites. According to the wear volume and worn morphology, the composites with micro- and nano-HA particles

weight percent of 15 and 10 exhibit a low friction coefficient and good wear resistance.

5. Friction and wear mechanism is furrow and scratch when the content of micro- and nano-HA under 15 and 10 wt %, but there are surface rupture and delamination on the worn surface of HA/UHMWPE composites when the content of micro- and nano-HA particles is more than 15 and 10 wt %, and the wear debris increases with increasing content of HA particles.

In the future, significant efforts are still needed to study the biological performance of micro- and nano-HA/UHMWPE composites in joint implants.

ACKNOWLEDGMENT

The research is supported by the Fundamental Research Funds for the Central Universities (2013XK07), the National Natural Science Foundation of China (Grant No. 51275514), and the Tribology Science Fund of State Key Laboratory of Tribology (SKLTKF11A03).

REFERENCES

1. Xiong, D.; Ge, S. *Wear* **2001**, *250*, 242.
2. Barbour, P. S. M.; Stone, M. H.; Fisher, J. *Biomaterials* **1999**, *20*, 2101.
3. Xiong, D. *Mater. Lett.* **2005**, *59*, 175.
4. Hoste, J.; Voorn, B.; Peenings, A. *Polym. Bull.* **1997**, *38*, 485.
5. Xue, Y.; Wu, W.; Jacobs, O.; Schadel, B. *Polym. Test.* **2006**, *25*, 221.
6. Plumlee, K.; Schwartz, C. J. *Wear* **2009**, *267*, 710.
7. Gong, G. F.; Yang, H. Y.; Fu, X. *Wear* **2004**, *256*, 88.
8. Li, S. Y.; Li, D. G. *Mater. Lett.* **2014**, *134*, 99.
9. Ge, S.; Wang, S.; Huang, X. *Wear* **2009**, *267*, 770.
10. Xiong, D.; Lin, J.; Fan, D. *J Mater. Sci. Mater. Med.* **2007**, *18*, 2131.
11. Xiong, D. *Biomed. Mater.* **2006**, *1*, 175.
12. Puertolas, J. A.; Kurtz, S. M. *J. Mech. Behav. Biomed.* **2014**, *39*, 129.
13. Boon-Peng, C.; Hazizan, M. A.; Ramdziah, B. M. N. *Wear* **2013**, *297*, 1120.
14. Tai, Z. X.; Chen, Y. F.; An, Y. F.; Yan, X. B.; Xue, Q. *J. Tribol. Lett.* **2012**, *46*, 55.
15. Cao, S. F.; Liu, H. T.; Ge, S. R.; Wu, G. F. *J. Reinf. Plast. Compos.* **2011**, *30*, 347.
16. Ren, L.; Liu, C.; Li, Y. *Wear* **2004**, *256*, 21.
17. Subramani, C.; Mhashe, S. T.; Kathe, A. A.; Varadarajan, P. V.; Virendra, P.; Nandanathangam, V. *Nanotechnology* **2007**, *18*, 385.
18. McConnell, D.; Frajola, W. J.; Deamer, D. W. *Science* **1961**, *344*, 281.
19. Durrieu, M. C.; Pallu, S.; Guillemot, F.; Bareille, R.; Amedee, J.; Baquey, C.; Labrugere, C.; Dard, M. *J Mater. Sci. Mater. Med.* **2004**, *15*, 779.
20. Lee, H. J.; Choi, H. W.; Kim, K. J.; Lee, S. C. *Chem. Mat.* **2006**, *18*, 5111.
21. Fang, L. M.; Leng, Y.; Gao, P. *Biomaterials* **2006**, *27*, 3701.

22. Wunderlich, B.; Cormier, C. M. *J. Polym. Sci. Part A-2*, **1967**, 5, 830.
23. Kang, X. Q.; Ge, S. R.; Dai, X. F. *Polym. Polym. Compos.* **2014**, 22, 561.
24. Xiong, D. S.; Lin, J. M.; Fan, D. L.; Jin, Z. M. *J Mater. Sci. Med.* **2007**, 18, 2131.
25. Gulmine, J. V.; Janissek, P. R.; Heise, H. M.; Akcelrud, L. *Polym. Test.* **2002**, 21, 557.
26. Gou, Y. C.; Feng, L.; Zhang, Y.; Song, L. L.; Ruan, J. Z. *Res. Exploration Lab.* **2011**, 30, 17.
27. Edidin, A. A.; Jewett, C. W.; Kalinowski, A.; Kwarteng, K.; Kurtz, S. M. *Biomaterials* **2000**, 21, 1451.
28. Xue, Q. J.; Wang, Q. H. *Wear* **1997**, 213, 54.
29. Tong, J.; Ma, R. D.; Arnell, R. D.; Ren, L. *Compos. Part A: Appl. S* **2006**, 37, 38.
30. Klaus, F.; Stoyko, F.; Zhong, Z. Springer, New York, **2005**.
31. Xiong, L.; Xiong, D. S.; Yang, Y. Y.; Jin, J. B. *J. Biomed. Mater. Res.* **2011**, 98, 127.
32. Schwartz, C. J.; Bahadur, S.; Mallapragada, S. K. *Wear* **2007**, 263, 1072.